Role of Aspartate-133 and Histidine-458 in the Mechanism of Tryptophan Indole-Lyase from *Proteus vulgaris*†

Tatyana V. Demidkina,‡ Lyudmila N. Zakomirdina,‡ Vitalia V. Kulikova,‡ Irene S. Dementieva,‡,$ Nicolai G. Faleev,§ Luca Ronda,|| Andrea Mozzarelli,|| Paul D. Gollnick⊥, and Robert S. Phillips*,#

Engelhardt Institute of Molecular Biology, Russian Academy of Sciences, 32 Vavilov Street, Moscow 119991, Russia, Nesmeyanov Institute of Organo-Element Compounds, Russian Academy of Sciences, 28 Vavilov Street, Moscow 117813, Russia, Department of Biochemistry and Molecular Biology, National Institute for the Physics of Matter, University of Parma, 43100, Parma, Italy, Department of Biological Sciences, State University of New York at Buffalo, Buffalo, New York 14260, USA, and Departments of Chemistry and of Biochemistry and Molecular Biology and Center for Metalloenzyme Studies, University of Georgia, Athens, Georgia 30602-2556 USA

Received March 4, 2003; Revised Manuscript Received July 25, 2003

ABSTRACT: Tryptophan indole-lyase (Trpase) from *Proteus vulgaris* is a pyridoxal 5′-phosphate dependent enzyme that catalyzes the reversible hydrolytic cleavage of L-Trp to yield indole and ammonium pyruvate. Asp-133 and His-458 are strictly conserved in all sequences of Trpase, and they are located in the proposed substrate-binding region of Trpase. These residues were mutated to alanine to probe their role in substrate binding and catalysis. D133A mutant Trpase has no measurable activity with L-Trp as substrate, but still retains activity with *S*-(*o*-nitrophenyl)-L-cysteine, *S*-alkyl-L-cysteines, and *β*-chloro-L-alanine. H458A mutant Trpase has 1.6% of wild-type Trpase activity with L-Trp, and high activity with *S*-(*o*-nitrophenyl)-L-cysteine, *S*-alkyl-L-cysteines, and *β*-chloro-L-alanine. H458A mutant Trpase does not exhibit the pK_a of 5.3 seen in the pH dependence of k_{cat}/K_m of L-Trp for wild-type Trpase. Both mutant enzymes are inhibited by L-Ala, L-Met, and L-Phe, with K_i values similar to those of wild-type Trpase, but oxindolyl-L-alanine and *β*-phenyl-DL-serine show much weaker binding to the mutant enzymes, suggesting that Asp-133 and His-458 are involved in the binding of these ligands. D133A and H458A mutant Trpase exhibit absorption and CD spectra in the presence of substrates and inhibitors that are similar to wild-type Trpase, with peaks at about 420 and 500 nm. The rate constants for formation of the 500 nm bands for the mutant enzymes are equal to or greater than those of wild-type Trpase, indicating that Asp-133 and His-458 do not play a role in the formation of quinonoid intermediates. In constrast to wild-type and H458A mutant Trpase, D133A mutant Trpase forms an intermediate from *S*-ethyl-L-Cys that absorbs at 345 nm, and is likely to be an α-aminoacrylate. Crystals of D133A and H458A mutant Trpase bind amino acids with similar affinity as the proteins in solution, except for L-Ala, which binds to D133A mutant Trpase crystals about 20-fold stronger than in solution. These results suggest that Asp-133 and His-458 play an important role in the elimination reaction of L-Trp. Asp-133 likely forms a hydrogen bond directly to the indole NH of the substrate, while His-458 probably is hydrogen bonded to Asp-133.

Tryptophan indole-lyase (also known as tryptophanase (Trpase)[1] [EC 4.1.99.1]) is a pyridoxal 5′-phosphate (PLP) dependent enzyme that catalyzes the reversible *β*-elimination reaction of L-Trp to form indole and ammonium pyruvate (eq 1).

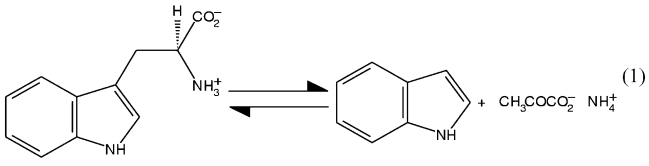

(1)

This enzyme has been found in a wide variety of Gram-negative bacteria, including *Escherichia coli* (*1*), *Proteus*

† Partial support for this work was provided by grants from NIH (GM42588) to R.S.P., from the Fogarty International Center (TW00106) to R.S.P. and T.V.D., from the Russian Foundation for Basic Investigations (01−04−48710) to L.N.Z., from the Howard Hughes Medical Institute (75195−54001) to T.V.D. and P.D.G., from a NATO−CLG (977117) to R.S.P., T.V.D., and A.M., and PRIN01 to A.M.

* To whom correspondence should be addressed at the Department of Chemistry, University of Georgia, Athens, GA 30602-2556 USA. Phone: (706) 542−1996. Fax: (706) 542−9454. E-mail: rsphillips@chem.uga.edu.

‡ Engelhardt Institute of Molecular Biology, Russian Academy of Sciences.

§ Nesmeyanov Institute of Organo-Element Compounds, Russian Academy of Sciences.

|| University of Parma.

⊥ State University of New York at Buffalo.

University of Georgia.

$ Current address: Biosciences Division, Structural Biology Center, Argonne National Laboratory, IL, 60439, USA.

[1] Abbreviations: Trpase, tryptophan indole-lyase, or tryptophanase [EC4.1.99.1]; TPL, tyrosine phenol-lyase [EC4.1.99.2]; PLP, pyridoxal-5′-phosphate; SOPC, *S*-(*o*-nitrophenyl)-L-cysteine; OIA, oxindolyl-L-alanine; *S*-Et-L-Cys, *S*-ethyl-L-cysteine; *S*-Me-L-Cys, *S*-methyl-L-cysteine; *S*-Bzl-L-Cys, *S*-benzyl-L-cysteine.

10.1021/bi034348t CCC: $25.00
Published on Web 09/05/2003

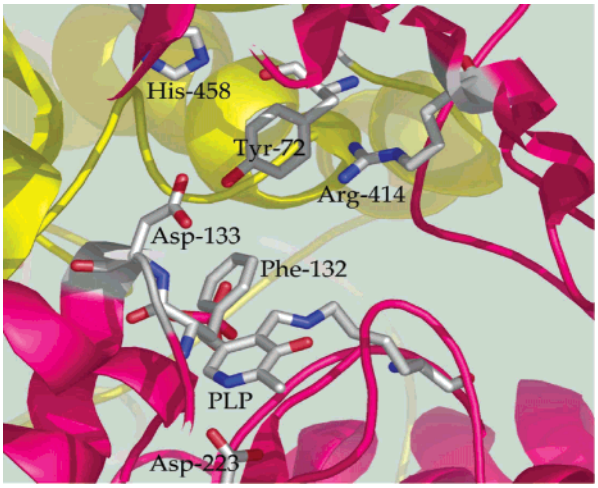

FIGURE 1: Active site of *Proteus vulgaris* Trpase, coordinates from 1AX4.pdb (*14*). This figure was prepared using PYMOL (*28*).

vulgaris (*2*), *Haemophilus influenza* (*3*), and *Vibrio cholera* (*4*). In the case of *H. influenza*, the virulence of the strain is associated with the presence of Trpase in the genome (*3*). Recently, it was shown that the *tna*A gene, encoding Trpase, is necessary for biofilm formation in *E. coli* (*5*). In addition to the physiological reaction shown in eq 1, Trpase can also catalyze the β-elimination reactions in vitro of a wide range of amino acids with suitable leaving groups on the β-carbon, including *S*-(*o*-nitrophenyl)-L-cysteine (*6*), *S*-alkyl-L-cysteines (*7*), β-chloro-L-alanine (*7*), L-serine (*7*), and *O*-acyl-L-serines (*8*). The mechanism of the enzyme from *E. coli* has been studied most extensively (*9*−*13*). However, the three-dimensional structure of the tetrameric enzyme from *P. vulgaris* has been determined by X-ray crystallography (*14*). The active site of Trpase, shown in Figure 1, is located at the interface of subunits in the dimer. Phe-132 has a π-stacking interaction with the PLP ring, which is connected to Lys-266 with a Schiff's base linkage, and forms a hydrogen-bond with Asp-223. Tyr-72 is likely to be a general acid catalyst, based on the results of mutagenesis of the corresponding Tyr in *E. coli* Trpase (*15*). Arg-414 is the α-carboxylate binding residue, based on sequence homology with other members of the aminotransferase family (*16*). Asp-133 and His-458 are basic residues located in the active site which could play a role in the catalytic mechanism. Comparison of the crystal structures of *P. vulgaris* Trpase (*14*) and of the very homologous tyrosine phenol-lyase from *Citrobacter freundii* (TPL) (*17*) shows that nearly all amino acid residues in the active sites are conserved. The structural and sequence alignment of *P. vulgaris* Trpase with that of *C. freundii* TPL shows that Phe-448 is found in *C. freundii* TPL in place of His-458, and Asp-133 in the structure of *P. vulgaris* Trpase is substituted by Thr-124 in the *C. freundii* TPL structure. These histidine-to-phenylalanine and aspartate-to-threonine substitutions are also seen in the sequence alignments of all known Trpase and TPL sequences. Recently, we demonstrated that Thr-124 and Phe-448 are important for the substrate specificity of *C. freundii* TPL for L-Tyr (*18*). Therefore, in the present work we performed site-directed mutagenesis of Asp-133 and His-458 to alanine in *P. vulgaris* Trpase, to determine the role of these residues in the catalytic mechanism and in the reaction specificity for L-Trp. The results suggest that both Asp-133 and His-458 in *P. vulgaris* Trpase are important for reaction specificity of L-Trp. In contrast, the binding and substrate activity of other amino acids is less affected by the mutations.

MATERIALS AND METHODS

General. L-Trp, *S*-ethyl-L-Cys (*S*-Et-L-Cys), *S*-benzyl-L-Cys (*S*-Bzl-L-Cys), and pyridoxal-5′-phosphate (PLP) were obtained from United States Biochemical Corporation. L-Ser, *S*-methyl-L-Cys (*S*-Me-L-Cys), β-phenyl-DL-Ser, and NADH were products of Sigma. *S*-(*o*-Nitrophenyl)-L-Cys (SOPC) was prepared as described previously (*19*). Oxindolyl-L-Ala (OIA) was prepared by oxidation of L-Trp as described previously (*9*).

Enzymes. Wild-type Trpase from *P. vulgaris* was prepared as described previously (*20*). H458A and D133A mutant *P. vulgaris* Trpases were prepared by site-directed mutagenesis. A 2.1-kb *Eco*RI−*Hind*III fragment from the pAVK2 plasmid was subcloned into pUC118 plasmid to create pID1. This insert contained the entire *tna*A gene that encodes tryptophanase from *P. vulgaris*, as well as part of the *tna*B gene encoding tryptophan permease (*2*). Single-stranded DNA was prepared from pID1 using M13K07 helper phage (*21*). The mutant proteins were created using a Sculptor in vitro mutagenesis kit (Amersham, Inc.). The mutagenic oligonucleotides were TTCCACTTTGCTACAACCG (for the Asp-133 to Ala mutation) and GTATTAAGAGCT TTACTGCAA (for the His-458 to Ala mutation), in which the underlined bases indicate the location of the mutation. Mutant clones obtained after the mutagenesis were screened by sequencing the gene in the mutated region using the Sequenase 2.0 kit from Amersham Life Science. The custom primers complementary to nucleotides 769−787 and 1828−1845 as defined in Kamath and Yanofsky (*2*) were used for sequencing the region of the plasmid containing the D133A and H458A mutations, respectively. *E. coli* SVS370 cells were used as the expression host for the plasmid, since these cells are *tna*A$^-$ and thus do not produce *E. coli* Trpase, which would interfere with assays for the mutant protein. The cells were grown and the mutant proteins were purified as previously described for wild-type Trpase (*20*).

Assays. The activity of Trpase and mutant forms was routinely measured with *S*-(*o*-nitrophenyl)-L-cysteine (SOPC) at 370 nm ($\Delta\epsilon = -1860$ M^{-1} cm^{-1}) in 0.05 M potassium phosphate, pH 8, containing 50 μM PLP, at 30 °C (*5*). β-Elimination activity with L-Trp, *S*-alkyl-L-cysteines, L-Ser, and β-chloro-L-Ala was measured with a lactate dehydrogenase coupled assay, following the absorbance decrease at 340 nm ($\Delta\epsilon = -6220$ M^{-1} cm^{-1}) (*22*). The reactions were performed at 30 °C in 0.05 M potassium phosphate, pH 8, containing 0.1 mM NADH and 20 μg/mL lactate dehydrogenase. For determination of V_{max} and V_{max}/K_m, the substrate concentration was varied, and the observed rates fitted to the hyperbolic form of the Michaelis−Menten equation (eq 2) with HYPERO (*23*). Values of k_{cat} and k_{cat}/K_m were calculated by dividing the fitted values of V_{max} and V_{max}/K_m by the concentration of enzyme, assuming a molecular mass of 52.7 kDa (*2*). All measurements of K_i were performed at 30° C in 0.1 M potassium phosphate, pH 7.8, containing 50 μM PLP and varying amounts of L-tryptophan or SOPC and inhibitors. K_i values were obtained by fitting the data to eq 3 using COMPO (*23*).

$$V = V_{max}[S]/(K_m + [S]) \quad (2)$$

$$V = V_{max}[S]/(K_m (1 + [I]/K_i) + [S]) \quad (3)$$

Stopped-Flow Kinetic Measurements. Stopped flow experiments were carried out using an RSM 1000 instrument from OLIS, Inc. equipped with a stopped flow mixing chamber. The stopped flow mixer has a 10-mm path length and a dead time of ca. 2 ms. Absorbance spectra were collected after flow stop over the wavelength range from 240 to 800 nm at a rate of 1000 spectra s^{-1}. Enzymes for stopped flow measurements were preincubated with excess PLP at 30 °C for 30 min, and then passed through a PD-10 (Pharmacia) gel filtration column equilibrated with 0.05 M potassium phosphate, pH 7.8, to remove excess PLP. The reactions were performed at 25.0 °C with the syringes immersed in a bath controlled by an external circulating Lauda water bath. The data were fitted using either single-wavelength or global analysis to the minimum number of exponentials required to obtain a reasonable fit, using the GlobalWorks software provided by OLIS (*24*). Global analysis of the data provides singular value decomposition (SVD) spectra which correspond to the global changes in the absorption spectrum for each phase of the reaction. The spectra shown in Figures 5 is the fitted SVD spectra corresponding to each phase of the reaction, not raw spectra for a particular time point.

Stopped flow data for formation of quinonoid intermediates at varying ligand concentration were fit to eq 4 (*25*), where k_f is the rate constant for formation of the quinonoid intermediate, and k_r is the rate constant for its reprotonation to return to the external aldimine. Equation 4 is derived for the mechanism shown in eq 5, where EA is the external aldimine and EQ is the quinonoid intermediate.

$$k_{obs} = 1/\tau = k_f[S]/(K_d + [S]) + k_r \quad (4)$$

$$E + S \underset{fast}{\overset{K_D}{\rightleftharpoons}} EA \underset{k_r}{\overset{k_f}{\rightleftharpoons}} EQ \quad (5)$$

Crystallization. Crystallization of H458A and D133A mutant Trpase was performed as previously described for wild-type Trpase from *P. vulgaris* (*14*, *26*).

Microspectrophotometric Measurements. Polarized absorption spectra were recorded at 20 °C with a Zeiss MPM03 UV−Vis microspectrophotometer equipped with ×10 objectives, as described previously (*26*). A Glan-Thompson polarizer is used to obtain linearly polarized light, and an analyzer is used to orient the crystal. Polarized absorption spectra were recorded on crystals suspended within a flow-cell in solutions containing 50% poly(ethylene glycol) 2000 monomethyl ether, 50 mM triethanolamine, 0.1 M KCl, 0.2 mM PLP, pH 8.01, 15 °C, and either ligands or substrates.

RESULTS AND DISCUSSION

His-458 and Asp-133 are located in the putative active site of *P. vulgaris* Trpase (Figure 1). These residues are strictly conserved in all known amino acid sequences of Trpase (Figure 2), as well as in many homologous sequences from microbial genomes. In TPL sequences, Asp-133 is aligned with Thr-124, and His-458 is replaced by Phe-448 (Figure 2). In previous studies with *C. freundii* TPL, we found that Thr-124 and Phe-448 are important for substrate specificity for L-Tyr, but not for SOPC and other suitable substrates (*18*). In the present work, we performed the mutation of both Asp-133 and His-458 to alanine in *P. vulgaris* Trpase to determine the role of these residues as potential acid−base catalysts in the mechanism of L-Trp elimination.

Activity of H458A and D133A Mutant Trpases. H458A mutant Trpase exhibits low, but easily measurable, activity with L-Trp as substrate, about 1.6% of wild-type for k_{cat} and 0.2% for k_{cat}/K_m (Table 1). H458A mutant Trpase exhibits primary and solvent isotope effects on k_{cat} (2.2 and 2.8, respectively) and k_{cat}/K_m (1.5 and 2.3, respectively), less than those observed on k_{cat} (3.8 and 3.6, respectively) and k_{cat}/K_m (2.4 and 3.4, respectively) for wild-type *P. vulgaris* Trpase (Table 1). In contrast, D133A mutant Trpase has no detectable elimination activity with L-Trp as substrate. The values of k_{cat} with SOPC, L-Ser, alkyl-L-cysteines, and β-chloro-L-Ala are equal to or greater than wild-type for H458A mutant Trpase (Table 1). Other substrates, SOPC, L-Ser, *S*-alkyl-L-cysteines and β-Cl-L-Ala, have significantly higher values of k_{cat}/K_m, ranging from 2- to 50-fold, for H458A mutant than wild-type enzyme (Table 1). This increase in activity is particularly striking for *S*-Bzl-L-Cys, which exhibits about a 50-fold increase in k_{cat}/K_m, due to a 3-fold increase in k_{cat} and a 15-fold decrease in K_m. Although k_{cat} decreases for most substrates with D133A mutant Trpase, it is more than compensated by corresponding decreases in K_m, so k_{cat}/K_m values for these substrates are comparable or greater for the D133A mutant than wild-type Trpase (Table 1).

Since there is measurable activity of H458A mutant Trpase with L-Trp, it was possible to determine the pH dependence of the kinetic parameters, k_{cat} and k_{cat}/K_m. Previous pH dependence experiments with wild-type *E. coli* Trpase found that k_{cat} is pH independent in the pH range 5.5−9.5, while k_{cat}/K_m exhibits pK_a values of 7.6 and 6.0 (*10*). The major difference in the pH dependence of wild-type and H458A mutant Trpase is the loss of the pK_a of 5.3 in the pH dependence of k_{cat}/K_m (Table 2), accompanied by a shift of the pK_a at 8.3 in wild-type to 7.9 for the mutant protein. The H463F mutant of *E. coli* Trpase was also found previously to lose the pK_a of 6 in the pH profile of k_{cat}/K_m (*15*). Since there was no detectable activity of D133A Trpase with L-Trp, the pH dependence for this mutant enzyme was measured with *S*-Et-L-Cys as substrate. The pH dependencies of k_{cat}/K_m for wild-type and D133A Trpase with *S*-Et-L-Cys are similar, with D133A being slightly higher throughout the pH range (Figure 3A). The pK_a's for the reaction of wild-type and D133A Trpase with *S*-Et-L-Cys are similar, 7.43 and 7.82, respectively (Table 2). The pH dependence of k_{cat} is strikingly different for wild-type and D133A Trpase, however. The value of k_{cat} increases with increasing pH for wild-type Trpase, with a pK_a of 6.66, while k_{cat} decreases with increasing pH for D133A Trpase, with a pK_a of 7.82 (Figure 3B).

Inhibition of H458A and D133A Mutant Trpases. H458A mutant Trpase is inhibited by L-Ala, L-Phe, and L-Met with similar K_i values to those for wild-type enzyme; however, OIA and β-phenyl-DL-Ser have K_i values which are raised 67- and 34-fold, respectively (Table 3). Thus, His-458 must be involved in the binding interactions of OIA and β-phenyl-

```
hflutna      EREKGLDRSKMVVFSNYFFDTTQGHSQINGATVRNVYIKEAFDTTAKHPFKGNFDLEKLE
ecoli        EQEKGLDRSKMVAFSNYFFDTTQGHSQINGCTVRNVYIKEAFDTGVRYDFKGNFDLEGLE
vcholera     EKEKGLDRSKMVALSNYFFDTTQGHTQINCCVAKNVYTEEAFDTGVKADFKGNFDLEKLE
pvulgaris    QKEGK..AKNPVFISNFHFDTTAAHVELNGCKAINIVTEKAFDSETYDDWKGDFDIKKLK
pinconstans  QEQGG..AKKPVFISNFHFDTTAAHVELNHCKAINIVTEKAYDSDTYDDWKGNFDIQKLK
entaer       ....K..SAHPVFISNFHFDTTAAHVELNGAKAINVVTPKAFDTTSWYDWKGNFDIDLLK
sttna1       ......TRPGMYVLSNMFFDTTRGHVQLGGRP.VDLLIDVPTEE..YHPFKGNMDTERLE
sttna2       ......TRPGMYVLSNMFFDTTRGHVQLAGRP.IDLLLDVPTEE..YHPFKGNMDTARLE
cfrtpl       ......IKPGQYVAGNMYFTTTRYHQEKNGAVFVDIVRDEAHDAGLNIAFKGDIDLKKLQ
eherbtpl     ......IKPGQYVAGNMYFTTTRFHQEKNGATFVDIVRDEAHDASLNLPFKGDIDLNKLA
sttpl        ......IKPGDYIPGNMYFTTTRTHQELQGGTFVDVIIDEAHDPQANHPFKGNVDIAKFE
             ..............N..F.TT..H.......................KG..D.....
             121.....130.......140.......150.......160.......170........

hflutna      LLRLTVPRATYTQTHMDFIIEAFQKVKENAENIKGLTFTYEPKVLRHFTARLKEVE
ecoli        LLRLTIPRATYTQTHMDFIIEAFKHVKENAANIKGLTFTYEPKVLRHFTAKLKEV
vcholera     LLRLTIPRATYTQTHMDFIIEAFEKVKANARNVKGLEFTYEPPVLRHFTARLKEKA
pvulgaris    FMRLTIARRVYTNDHMDYIADALIGLKEKFATLKGLEFEYEPPVLRHFTARLKPIE
pinconstans  FMRLTIARRVYTNDHMDYIADALIGLKDKFATLKGLDFEYEPPVLRHFTARLKPIK
entaer       LLRLTIPRRVYTNDHMDYIADALIAVKARAATIKGLTFTYEPPVLRHFVARLKPVK
sttna1       FTRLAIPRRVYTNLHLEDVAETVINAFQKREEIRGVKFAREPKVLRHFTAWFDPA
sttna2       FTRLAIPRRVYTNLHLEDVAETVINAFQKREQIRGVKFTREPKVLRHFTAHFDLV
cfrtpl       TVRLTIPRRVYTYAHMDVVADGIIKLYQHKEDIRGLKFIYEPKQLRFFTARFDYI
eherbtpl     TVRLTIPRRVYTYAHMDVVADGIIKLYQHKEDIRGLTFVYEPKQLRFFTARFDFI
sttpl        LVRLTIPRRVYTDRHMDVVAYSVKHLWKERDTIRGLRMVYEPPTLRFFTARFEPIS
             ..RL...R..YT..H...................GL....EP..LR.F.A......
             421.....430.......440.......450.......460.......470....
```

FIGURE 2: Partial sequence alignments of Trpase and TPL. The sequences are from *Haemophilus influenza* Trpase (hflutna), *Escherichia coli* K-12 Trpase (ecoli), *Vibrio cholera* Trpase (vcholera), *Proteus vulgaris* Trpase (pvulgaris), *Proteus inconstans* Trpase (pinconstans), *Enterobacter aerogenes* Trpase (entaer), *Symbiobacterium thermophilum* Trpase 1 (sttna1), *Symbiobacterium thermophilum* Trpase 2 (sttna2), *Citrobacter freundii* TPL (cfrtpl), *Erwinia herbicola* TPL (eherbtpl), and *Symbiobacterium thermophilum* TPL (sttpl). The consensus sequence is shown below. Asp-133 (consensus residue 140) and His-458 (consensus residue 467) are shown in bold.

Table 1: Steady-State Kinetic Parameters for Wild-Type, H458A, and D133A Mutant Trpase

	wild type			H458A			D133A		
substrate	K_m, mM	k_{cat}, s^{-1}	k_{cat}/K_m, M^{-1} s^{-1}	K_m, mM	k_{cat}, s^{-1}	k_{cat}/K_m, M^{-1} s^{-1}	K_m, mM	k_{cat}, s^{-1}	k_{cat}/K_m, M^{-1} s^{-1}
L-Trp	0.28	6.29	2.25×10^4	1.15	0.11	9.5×10^1	*a*	$<10^{-5}$	*a*
L-Trp(D_2O)	0.26	1.73	6.65×10^3	1.0	0.04	4.0×10^1	*a*	*a*	*a*
H^2-L-Trp	0.18	1.66	9.32×10^3	0.76	0.05	6.5×10^1	*a*	*a*	*a*
SOPC	0.18	33.35	1.85×10^5	0.1	31.8	3.18×10^5	0.01	1.4	1.40×10^5
L-Ser	50.9	1.83	3.59×10^1	7.85	1.3	1.65×10^2	*b*	*b*	*b*
S-Me-L-Cys	16.8	4.1	2.38×10^2	2.32	6.03	2.59×10^3	0.19	0.35	1.84×10^3
S-Et-L-Cys	3.17	3.59	1.13×10^3	0.42	6.41	1.52×10^4	0.03	0.21	7.0×10^3
S-Bzl-L-Cys	0.8	1.95	2.44×10^3	0.096	10.9	1.13×10^5	0.01	0.87	8.70×10^4
β-Cl-L-Ala	9.36	8.41	8.98×10^2	5.6	23.3	4.16×10^3	4.6	10.8	2.35×10^3

[a] No detectable activity. [b] Not determined.

Table 2: Apparent pK_a Values of the Kinetic Parameters for Reactions of Wild-Type and Mutant Trpase

enzyme	wild-type		H458A	D133A
substrate	L-Trp	*S*-Et-L-Cys	L-Trp	*S*-Et-L-Cys
k_{cat}	6.52 ± 0.16	6.66 ± 0.06	6.73 ± 0.14	7.82 ± 0.16
k_{cat}/K_m	8.3 ± 0.13	7.43 ± 0.12	7.86 ± 0.14	7.82 ± 0.05
	5.32 ± 0.25			

DL-Ser. OIA was previously prepared as a possible transition-state analogue inhibitor for the indole elimination step of Trpase (*9*), so it would be expected that mutations that affect indole elimination from L-Trp would have a similar effect on inhibitor binding.

Inhibition of D133A mutant Trpase could not be measured with L-Trp, since it is not a substrate, but could be measured with SOPC. For OIA and β-phenyl-DL-Ser, it was found that there is about a 10-fold difference between the K_i values measured with L-Trp and SOPC for wild-type Trpase (Table 3). The reason for this difference is unclear at this time. There are only modest effects on L-Ala and L-Phe inhibition, but the binding of L-Met is strongly increased, more than 60-fold, in D133A mutant Trpase. In contrast, the binding of OIA is much weaker for D133A mutant Trpase (Table 3), as expected for a possible transition-state analogue inhibitor (*9*) binding to an enzyme with a compromised catalytic site. Inhibition by β-phenyl-DL-Ser is also severalfold weaker for D133A mutant Trpase than wild-type enzyme, suggesting a role for Asp-133 in β-phenyl-DL-Ser binding.

Absorption and CD Spectra of H458A and D133A Mutant Trpases. Wild-type and both mutant enzymes exhibit absorption peaks at about 420 nm for the internal aldimines. The corresponding CD spectra exhibit positive bands (Figure 4A). The anisotropy factors values ($\Delta A/A$) of this band for the wild type, D133A and H458 mutant enzymes are equal to 25.6×10^{-4}, 30.5×10^{-4}, and 11.2×10^{-4}, respectively. Thus, the spectroscopic properties of the internal aldimines of the mutants are similar, but not identical, to those of the

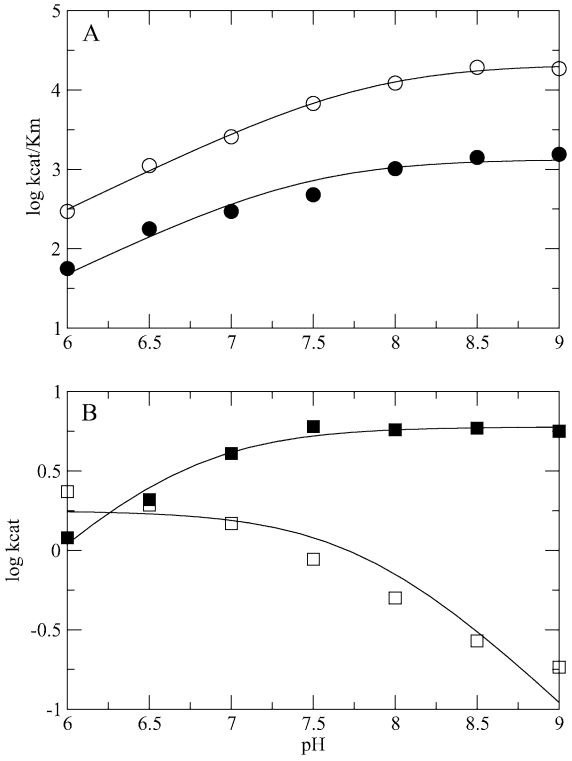

FIGURE 3: pH dependence of k_{cat} and k_{cat}/K_m for wild-type and D133A mutant Trpase with *S*-Et-L-Cys. (A) pH dependence of k_{cat}/K_m for wild-type (filled circles) and D133A mutant Trpase (open circles). (B) pH dependence of k_{cat} for wild-type (filled squares) and D133A mutant Trpase (open squares). The lines are the fitted lines with the pK_a's given in Table 2.

wild-type Trpase. This suggests that the microenvironment of the internal aldimines in the mutant enzymes is different than that in the wild-type enzyme.

L-Ala and OIA bind to wild-type Trpase from *P. vulgaris* to form predominantly quinonoid complexes with absorption maxima at 500 nm, and corresponding positive CD bands (*20*). Addition of L-Ala and OIA to both H458A and D133A mutant Trpases results in intense absorbance and positive CD bands at about 500 nm ascribed to quinonoid complexes, similar to those observed with wild-type Trpase (data not shown). With L-Phe and β-phenyl-DL-Ser, the enzyme does not form a significant amount of the 500 nm species, and external aldimine formation with these amino acids is accompanied by a sharp decrease of the positive CD band of the holoenzyme at 420 nm (Figure 4B,C).

In contrast to the negative CD band of the external aldimine of the wild-type enzyme with β-phenyl-DL-Ser, both D133A and H458A mutant Trpase show a positive CD band at 425 nm on interaction with β-phenyl-DL-Ser (Figure 4B). The opposite sign of the CD band at 425 nm in the H458A and D133A mutant enzymes complexed with β-phenyl-DL suggests that β-phenyl-DL-Ser may preferentially form a Michaelis complex, rather than an external aldimine, with H458A and D133A mutant Trpase. Alternatively, the external aldimine with β-phenyl-DL-Ser in the mutant enzymes may have a different electronic environment.

Unlike the wild-type enzyme, in the absorption and CD spectra of L-Phe with H458A and D133A mutant enzymes there are species with λ_{max} at 425 and 500 nm (Figure 4C). There is C-α-proton exchange in both mutant enzymes complexed with L-Phe (Table 5). The rate constants for α-proton exchange of L-Phe with wild-type, H458A, and D133A mutant Trpases are very similar, with the mutant enzymes slightly faster than wild-type (Table 5). Thus, L-Phe forms an equilibrium mixture of external aldimine and quinonoid complexes with both mutant Trpases. There is a significant difference in the values of the anisotropy factors for the 425 nm external aldimine band of the Phe complexes of the wild-type enzyme ($\Delta A/A = 1.0 \times 10^{-4}$) and for H458A ($\Delta A/A = 1.1 \times 10^{-3}$) and D133A ($\Delta A/A = 6.4 \times 10^{-4}$) mutant Trpase.

Thus, the spectroscpic data allow us to propose that the conformations of the external aldimines of the mutant enzymes with β-phenyl-DL-Ser and L-Phe differ from those of the wild-type enzyme, and this conformation, in the case of L-Phe, allows efficient C-α-proton abstraction, unlike the external aldimine conformation of L-Phe with the wild-type enzyme. This prediction is also consistent with the significantly weaker inhibition of H458A and D133A mutant Trpase by β-phenyl-DL-Ser, as discussed above.

Stopped-Flow Kinetic Studies of H458A and D133A Mutant Trpases. The formation of quinonoid intermediates from wild-type, H458A and D133A mutant Trpases with L-Ala, L-Met, *S*-Et-L-Cys, and OIA was followed by rapid-scanning stopped-flow spectrophotometry. D133A mutant Trpase reacts with L-Met (data not shown) to approach an equilibrium dominated by an intensely absorbing quinonoid complex, in a transient which exhibits three phases, with $1/\tau_1 = 96 \pm 20\ s^{-1}$, $1/\tau_2 = 32 \pm 5\ s^{-1}$, and $1/\tau_3 = 1.8 \pm 0.5\ s^{-1}$. The intermediate and final spectra show a slight shift in the absorption maximum of the quinonoid band. The formation of the quinonoid complex of L-Met with H458A mutant Trpase occurs in two phases, with $1/\tau_1 = 24.9 \pm 1.7\ s^{-1}$ and $1/\tau_2 = 3.7 \pm 0.2\ s^{-1}$. In comparison, wild-type Trpase reacts with L-Met to form a quinonoid species with two phases, with $1/\tau_1 = 10.2 \pm 1.6\ s^{-1}$ and $1/\tau_2 = 3.7 \pm 0.3\ s^{-1}$.

S-Et-L-Cys also reacts with wild-type, H458A, and D133A mutant Trpases to form quinonoid intermediates, as shown from the SVD spectra in Figure 5. Since *S*-Et-L-Cys is a substrate, these reactions are approaches to steady-state rather than to equilibrium. However, it is interesting that the quinonoid intermediates with *S*-Et-L-Cys of both H458A and D133A mutant Trpases (compare time courses at 506 nm in Figure 5B,D,F) form nearly 10-fold faster than wild-type Trpase ($324 \pm 5\ s^{-1}$ for D133A and $310 \pm 30\ s^{-1}$ for H458A vs $36 \pm 3\ s^{-1}$ for wild-type). The increase in the rate constants for quinonoid intermediate formation is likely responsible for the increase in k_{cat}/K_m of *S*-Et-L-Cys for H458A and D133A mutant Trpase compared with wild-type Trpase (Table 1). It is particularly interesting that the initial quinonoid intermediate formed from *S*-Et-L-Cys with D133A mutant Trpase decays rapidly, with $1/\tau = 4.0 \pm 0.2\ s^{-1}$, to form a new intermediate with an absorption peak at 345 nm (Figure 5A, dashed and double dotted line), that is likely to be an aminoacrylate. An aminoacrylate intermediate, with identical spectroscopic properties, which forms with a rate constant of $6\ s^{-1}$, was previously observed in the reaction of wild-type *E. coli* Trpase with *S*-Et-L-Cys and L-Trp, but only in the presence of 5 mM benzimidazole, an uncompetitive inhibitor that binds selectively to the aminoacrylate intermediate (*12*). Both wild-type and H458A *P. vulgaris* Trpase form a similar 345 nm intermediate from *S*-Et-L-Cys

Table 3: Competitive Inhibition of Wild-Type and H458A and D133A Mutant Trpase by Amino Acids

	K_i, mM			
inhibitor	wild-type (Trp)	wild-type (SOPC)	H458A (Trp)	D133A (SOPC)
L-Ala	24.5 ± 2.08	28.19 ± 2.49	24.0 ± 2.5	6.37 ± 0.87
OIA	0.003 ± 0.00003	0.03 ± 0.003	0.2 ± 0.01	2.80 ± 0.32
L-Phe	4.6 ± 0.3	9.17 ± 0.90	9.1 ± 0.5	7.9 ± 0.89
β-phenyl-DL-Ser	0.71 ± 0.05	9.76 ± 0.92	23.9 ± 1.8	35.0 ± 6.0
L-Met	6.57 ± 0.7	7.65 ± 0.71	3.98 ± 0.28	0.1 ± 0.015

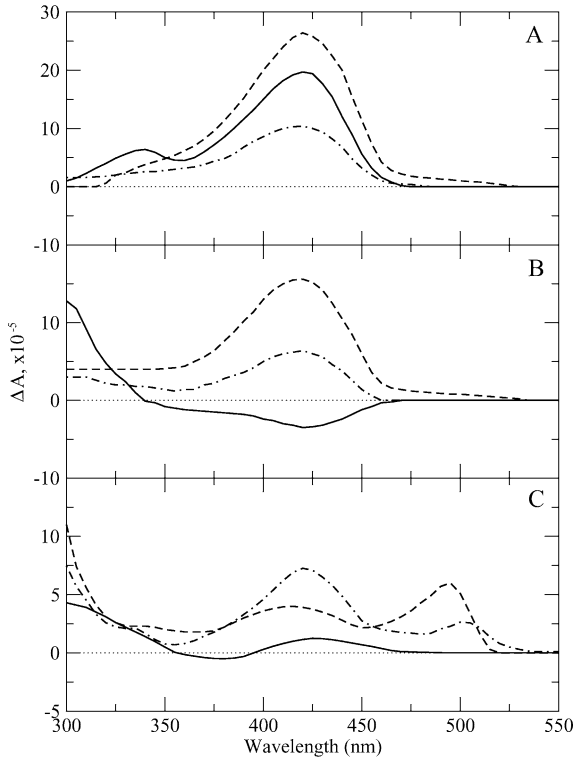

FIGURE 4: Circular dichroism spectra of wild-type, H458A and D133A mutant Trpase. (A) Wild-type Trpase (−); D133A mutant Trpase (- - -); H458A mutant Trpase (−•−). (B) Wild-type Trpase complexed with β-phenyl-DL-Ser (−); D133A mutant Trpase complexed with β-phenyl-DL-Ser (- - -); H458A mutant Trpase complexed with β-phenyl-DL-Ser (−•−). (C) Wild-type Trpase complexed with L-Phe (−); D133A mutant Trpase complexed with L-Phe (- - -); H458A mutant Trpase complexed with L-Phe (−•−).

in the presence of 5 mM benzimidazole (data not shown). In contrast, 5 mM benzimidazole has no effect on the spectrum in the reaction of D133A mutant Trpase (data not shown). Thus, since an apparent aminoacrylate accumulates in the reaction of D133A mutant Trpase, and the k_{cat} for *S*-Et-L-Cys is reduced by about an order of magnitude compared with H458A and wild-type Trpase, the rate-limiting step appears to be changed from thiol elimination, in wild-type Trpase (*12*), to pyruvate release, by the mutation of Asp-133 to alanine. A change in rate-determining step is also consistent with the dramatic difference in the pH dependence of k_{cat} seen for wild-type and D133A Trpase (Figure 2B).

The reaction of wild-type and H458A Trpase with OIA results in the appearance of an intense absorption band at 500 nm, but no significant absorbance attributable to the external aldimine is observed (data not shown). The kinetics of the appearance of the quinonoid intermediate for wild-type Trpase is described by three exponential processes. The first and third phases are concentration independent, with $1/\tau_1 = 49 \pm 13$ s^{-1} and $1/\tau_3 = 3.4 \pm 0.9$ s^{-1}. The second phase of the reaction is concentration-dependent, with the dependence being described by eq 4, with $K_d = 2.7 \pm 0.6$ mM, $k_f = 63 \pm 5$ s^{-1}, and $k_r = 0$ (Table 4). These values, however, cannot be considered as reflecting directly the formation of the external aldimine and its deprotonation. The rate constant for the formation of the quinonoid intermediate of OIA with H458A Trpase is similar to that of wild-type (Table 4), but the apparent binding is 5-fold weaker.

The approach to steady-state of L-Trp with wild-type *P. vulgaris* Trpase is described by two exponential processes, the second one of which is independent of [L-Trp], with $1/\tau_2 = 3.4 \pm 1.4$ s^{-1}. The parameters obtained from fitting of the [L-Trp] dependence of the first, faster exponential process are presented in Table 4. In the reaction of H458A Trpase with L-Trp, there are also two exponential processes. The slow second phase (with $1/\tau_2 = 4.1 \pm 1.4$ s^{-1}) is independent of [L-Trp], and the initial fast phase shows a dependence on [L-Trp]. The kinetic parameters obtained from the dependence of $1/\tau_1$ on [L-Trp] are presented in Table 4. The effective binding efficiencies, reflecting the formation of the external aldimine, and subsequent deprotonation to quinonoid intermediates, were calculated using eq 6.

$$K_{eff} = K_d/(1 + k_f/k_r) \quad (6)$$

For reactions of H458A Trpase with OIA and wild-type enzyme with L-Trp, the calculated values of K_{eff} were 0.24 and 0.31 mM, which agree well with the respective values of K_i and K_m found in steady-state experiments. However, for the reaction of H458A Trpase with L-Trp, the real K_m (1.15 mM) is considerably larger than the predicted K_{eff} (0.32 mM).

Binding of Amino Acids to Crystals of H458A and D133A Mutant Trpase. D133A and H458A mutant Trpase readily form crystals under the conditions used to crystallize wild-type Trpase (*14*, *26*). Previously, we examined the binding of OIA and other amino acids to crystals of wild-type Trpase from *P. vulgaris*, and we found that they bind amino acids with apparent binding constants about an order of magnitude higher than the enzyme in solution (*26*). In the present study, we examined the binding of L-Ala, L-Phe, L-Trp, and OIA to the mutant protein crystals by microspectrophotometry. The crystals of H458A and D133A mutant Trpase react with L-Ala, L-Phe, L-Trp, and OIA to form equilibrating mixtures of external aldimine and quinonoid intermediates, similar to what we found previously with wild-type Trpase (*26*). Titration of the crystals provides the apparent binding constants for the ligands. The titration of D133A mutant Trpase with L-Ala is shown in Figure 6. The results of the titrations are given in Table 6. The K_i values for L-Phe and OIA are similar for solution (Table 3) and the crystals (Table 6) of D133A and H458A mutant Trpase. However, L-Ala binds much better to D133A than H458A mutant Trpase

Table 4: Pre-Steady-State Kinetic Constants for Wild-Type and H458A Mutant Trpase

	wild-type			H458A		
amino acid	K_d, mM	k_f, s^{-1}	k_r, s^{-1}	K_d, mM	k_f, s^{-1}	k_r, s^{-1}
L-Trp	1.06 ± 0.9	109.5 ± 16.3	45.3 ± 18.1	6.52 ± 1.61	109 ± 10	5.3 ± 2.2
OIA	2.7 ± 0.6	63 ± 5	$\cong 0$	10.66 ± 3.23	45.25 ± 9.55	1.06 ± 0.22

Table 5: Isotope Exchange Rates in ^2H_2O for Wild-Type, H458A and D133A Mutant Trpase

	L-Phe		
	wild-type	H458A	D133A
k_{exch}, s^{-1}	0.68	0.89	1.1

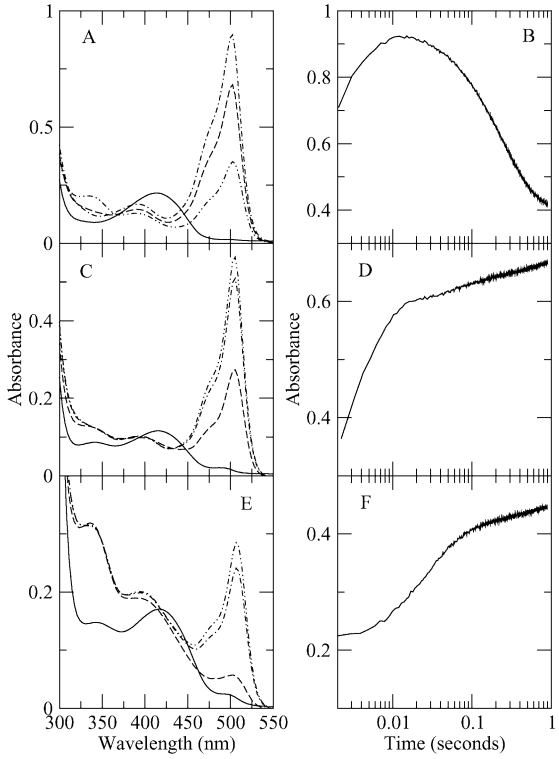

FIGURE 5: Rapid-scanning stopped-flow reaction of D133A, H458A, and wild-type Trpase with *S*-Et-L-Cys. (A) D133A reaction with 20 mM *S*-Et-L-Cys. D133A mutant Trpase, solid line; first SVD spectrum, dashed line; second SVD spectrum, dashed and dotted line; third SVD spectrum, dashed and double dotted line. (B) Time course of the reaction in A at 502 nm. (C) H458A Trpase reaction with 20 mM *S*-Et-L-Cys. D133A mutant Trpase, solid line; first SVD spectrum, dashed line; second SVD spectrum, dashed and dotted line; third SVD spectrum, dashed and double dotted line. (D) Time course of the reaction in C at 502 nm. (E) Wild-type Trpase reaction with 20 mM *S*-Et-L-Cys. Wild-type Trpase, solid line; first SVD spectrum, dashed line; second SVD spectrum, dashed and dotted line; third SVD spectrum, dashed and double dotted line. (F) Time course of the reaction in E at 502 nm.

crystals, and, surprisingly, the binding of L-Ala to the crystals of D133A mutant Trpase is about 20-fold stronger than in solution. Generally, it has been observed that the binding of ligands to protein crystals is weaker than in solution (*27*). In the case of the L-Ala complex of D133A mutant Trpase, it is possible that crystal lattice interactions stabilize the conformation of the complex. The strong binding and high stability of the D133A−L-Ala complex makes it particularly suitable for analysis by X-ray crystallography.

What Are the Mechanistic Roles of Asp-133 and His-458 in Trpase Catalysis? Mutation of both Asp-133 and His-458 results in significant loss of catalytic activity with L-Trp, and mutation of Asp-133 also affects the activity of non-physiological substrates (Table 1). Furthermore, D133A Trpase accumulates an intermediate with λ_{max} at 345 nm, likely an aminoacrylate, which is not seen with wild-type or H458A enzymes (Figure 5). Thus, Asp-133 is a more critical residue for activity. The mutant enzymes readily form quinonoid complexes (Figures 4−6), exhibit a pK_a of about 7.8 in pH dependence of k_{cat}/K_m (Table 2), and can catalyze α-hydrogen exchange (Table 5). Thus, neither His-458 nor Asp-133 is the base needed for α-deprotonation. In earlier work, we identified a base with a pK_a of 6 in the pH dependence of k_{cat}/K_m for *E. coli* Trpase that was necessary for reaction of L-Trp, but not for *S*-Me-L-Cys (*10*). This base was also observed in the pH dependence of inhibition by OIA, suggesting that it plays a role in the binding of this compound (*10*). Wild-type *P. vulgaris* Trpase shows a similar pH dependence in the reaction of L-Trp, with a pK_a of 5.3 (Table 2). The pH dependence of the reaction of H458A

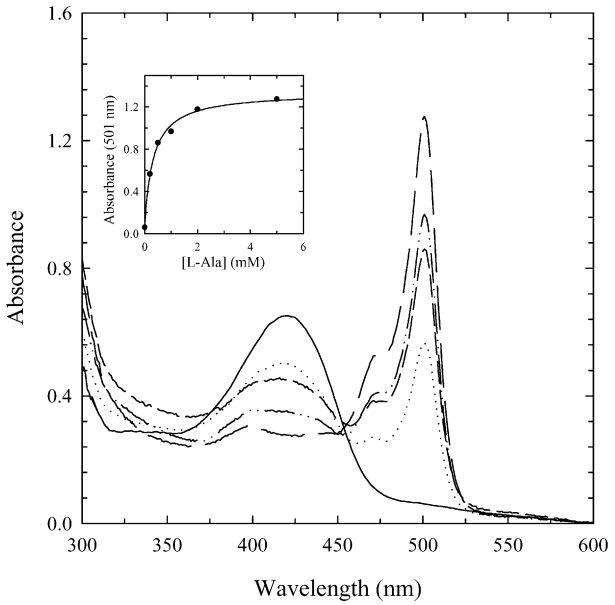

FIGURE 6: Titration of D133A mutant Trpase crystals with L-Ala. Polarized absorption spectrum of a crystal of D133A mutant Trpase suspended in a solution containing 50% poly(ethylene glycol) 2000 monomethyl ether, 50 mM triethanolamine, 0.1 M KCl, 0.2 mM PLP, pH 8.01, 15 °C, were recorded along the lower intensity direction, in the absence (−) and presence of increasing concentrations of L-Ala: 0.2 (...), 0.5 (−), 1.0 (−••−), 5 mM (− −). Inset: absorbance change at 501 nm as a function of L-Ala concentration. The solid line through the data points is the fit to a binding isotherm with dissociation constant of 0.33 ± 0.05 mM.

Table 6: Binding Constants of Amino Acids for Crystals of H458A and D133A Mutant Trpase

enzyme	[L-Ala], mM	[L-Phe], mM	[L-Trp], mM	[OIA], mM
H458A	8.92 ± 0.16	12.32 ± 1.42	*a*	0.64 ± 0.18
D133A	0.33 ± 0.05	3.60 ± 0.05	13.15 ± 1.03	1.01 ± 0.25

[a] Not determined.

Scheme 1

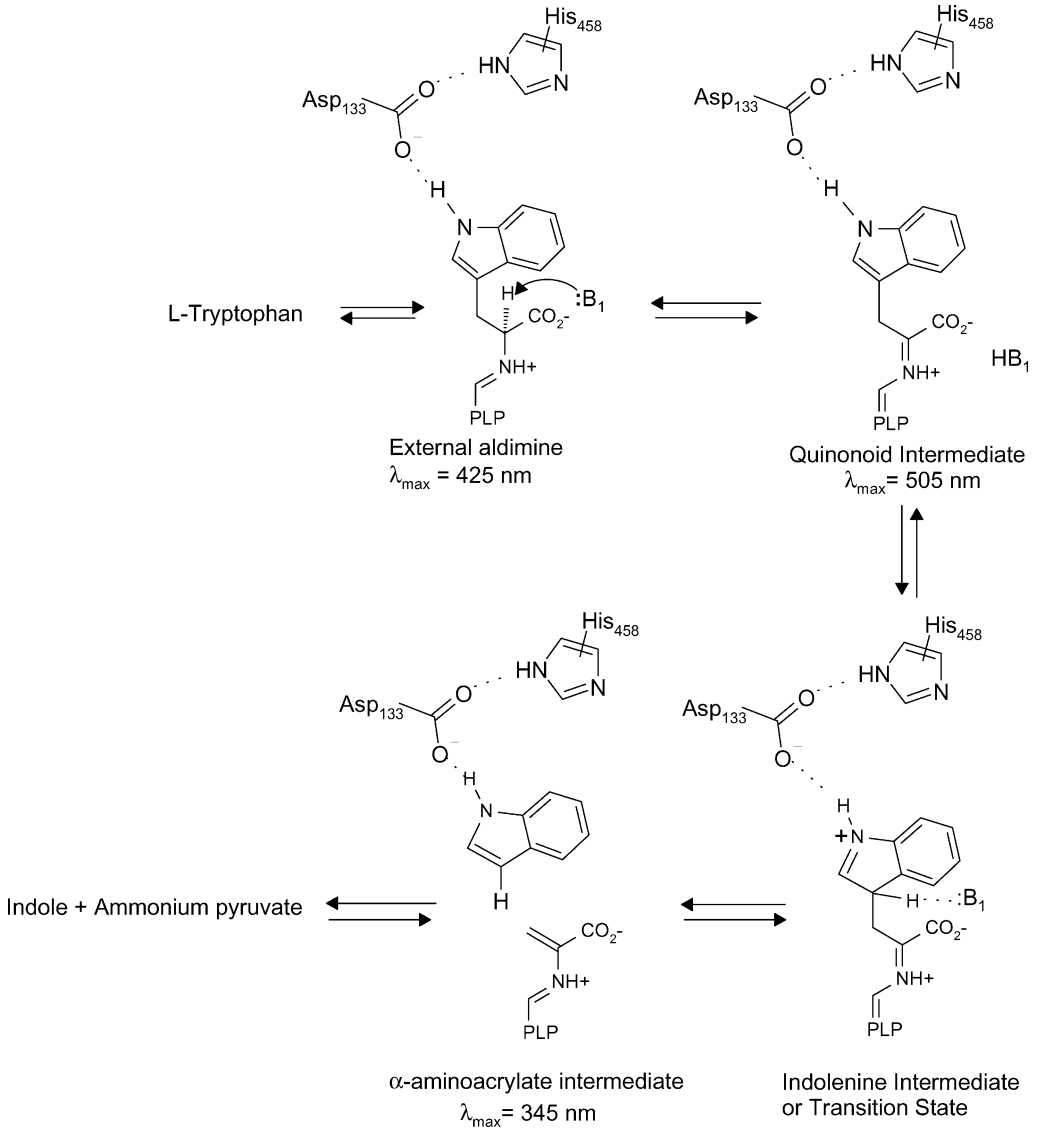

mutant Trpase with L-Trp does not exhibit the pK_a of 5.3 (Table 2). A similar result was previously observed with H463F *E. coli* Trpase (*15*). Thus, His-458 is either the basic group with pK_a of 5.3, or it influences that base such that its replacement perturbs the pK_a. It seems most likely that this base is the Asp-133-His-458 pair, which could form a hydrogen-bonded dimer. This dimer then can hydrogen bond, either by the Asp δ-O or the His δ-N, to the indole NH of the Trp substrate. This hydrogen bond appears to be necessary for efficient catalysis, as protonation of the base would preclude hydrogen bond formation to the substrate. Since the D133A mutant enzyme has negligible activity with L-Trp, it is most likely that Asp-133 is the residue which directly contacts the substrate. This conclusion is supported by the structure of the complex of *P. vulgaris* Trpase with OIA, which shows a hydrogen bond between Asp-133 and the oxindole NH (M. Isupov, personal communication). The proposed role of Asp-133 and His-458 in the mechanism of L-Trp elimination is illustrated in Scheme 1. Asp-133 hydrogen bonds to the indole NH of the substrate and to His-458. This interaction is necessary for efficient proton transfer to C_3, which may be concerted with C_3-C_β bond cleavage (*13*). Thus, D133A mutant Trpase shows no measurable elimination of indole from L-Trp, a decrease in k_{cat} of at least 5 orders of magnitude. Furthermore, Asp-133 also plays a role in the release of pyruvate from the aminoacrylate intermediate formed from *S*-Et-L-Cys, affects the PLP environment, and appears to have an influence on the crystal lattice interactions of the enzyme. It is not clear if these effects are related to the acid/base properties of Asp-133. In contrast, H458A mutant Trpase exhibits only a 60-fold reduction in k_{cat} with L-Trp, and exhibits some modest effects on the PLP environment. The role of His-458 then appears to be primarily as an auxiliary, possibly positioning Asp-133 for optimum interaction with the substrate during the transition state for indole elimination.

ACKNOWLEDGMENT

We thank Min Yang and Xiao-ping Chen for their helpful assistance in preparing the site-directed mutants.

REFERENCES

1. Morino, Y., and Snell, E. E. (1967) *J. Biol. Chem. 242*, 2800.
2. Kamath, A. V., and Yanofsky, C. (1992) *J. Biol. Chem. 267*, 19978.

3. Martin, K., Morlin, G., Smith, A., Nordyke, A., Eisenstark, A., and Golomb, M. (1998) *J. Bacteriol. 180*, 107.
4. Heidelberg, J. F., Eisen, J. A., Nelson, W. C., Clayton, R. A., Gwinn, M. L., Dodson, R. J., Haft, D. H., Hickey, E. K., Peterson, J. D., Umayam, L., Gill, S. R., Nelson, K. E., Read, T. D., Tettelin, H., Richardson, D., Ermolaeva, M. D., Vamathevan, J., Bass, S., Qin, H., Dragoi, I., Sellers, P., McDonald, L., Utterback, T., Fleishmann, R. D., Nierman, W. C., and White, O. (2000) *Nature 406*, 477.
5. Di Martino, P., Merieau, A., Phillips, R., Orange, N. and Hulen, C. (2002) *Can. J. Microbiol. 48*, 132−137.
6. Suelter, C. H., Wang, J., and Snell, E. E. (1976) *FEBS Lett. 66*, 230.
7. Watanabe, T., and Snell, E. E. (1977) *J. Biochem. (Tokyo) 82*, 733.
8. Phillips, R. S. (1987) *Arch. Biochem. Biophys. 256*, 302.
9. Phillips, R. S., Miles, E. W., and Cohen, L. A. (1984) *Biochem. 23*, 6228.
10. Kiick, D. M., and Phillips, R. S. (1988) *Biochem. 27*, 7333.
11. Phillips, R. S. (1989) *J. Am. Chem. Soc. 113*, 727.
12. Phillips, R. S. (1991) *Biochemistry 30*, 5927.
13. Phillips, R. S., Sundararaju, B., and Faleev, N. G. (2000) *J. Am. Chem. Soc. 122*, 1008−14.
14. Isupov, M. N., Antson, A. A., Dodson, E. J., Dodson, G. G., Dementieva, I. S., Zakomirdina, L. N., Wilson, K. S., Dauter, Z., Lebedev, A. A., and Harutyunyan, E. H. (1998) *J. Mol. Biol. 276*, 603.
15. Phillips, R. S., Johnson, N. and Kamath, A. V., (2002) *Biochemistry 41*, 4012−9.
16. Alexander, F. W., Sandmeier, E., Mehta, P. K., and Christen, P., (1994) *Eur. J. Biochem. 219*, 953−60
17. Sundararaju, B., Antson, A. A., Phillips, R. S., Demidkina, T. V., Barbolina, M. V., Gollnick, P., Dodson, G. G., and Wilson, K. S. (1997) *Biochemistry 36*, 6502.
18. Demidkina, T. V., Barbolina, M. V., Faleev, N. G., Sundararaju, B., Gollnick, P. D., and Phillips, R. S. (2002) *Biochem. J. 363*, 745−752.
19. Dua, R. K., Taylor, E. W., and Phillips, R. S. (1993) *J. Am. Chem. Soc. 115*, 1264.
20. Zakomirdina, L. N., Kulikova, V. V., Gogoleva, O. I., Dementieva, I. S., Faleev, N. G., and Demidkina, T. V. (2002) *Biochemistry (Moscow) 67*, 1189.
21. Vieira, J., and Messing, J. (1987) *Methods Enzymol. 153*, 1.
22. Morino, Y., and Snell, E. E. (1970) *Methods Enzymol. 17A*, 439.
23. Cleland, W. W. (1979) *Methods Enzymol. 63*, 103.
24. Matheson, I. B. C. (1990) *Comput. Chem. 14*, 49.
25. Strickland, S., Palmer, G., and Massey, V. (1975) *J. Biol. Chem. 250*, 4048.
26. Phillips, R. S., Demidkina, T. V., Zakomirdina, L. N., Bruno, S., Ronda, L. and Mozzarelli, A. (2002) *J. Biol. Chem. 277*, 21592.
27. Mozzarelli, A., and Rossi, G. L. (1996) *Annu. Rev. Biophys. Biomol. Struct. 25*, 343.
28. DeLano, W. L. (2002) The PyMOL Molecular Graphics System, DeLano Scientific, San Carlos, CA. http://www.pymol.org.

BI034348T